PHYSICAL REVIEW B VOLUME 50, NUMBER 23 15 DECEMBER 1994-I

Anomalous temperature dependence of the correlated $\nu=1$ quantum Hall effect in bilayer electron systems

T. S. Lay
Department of Electrical Engineering, Princeton University, Princeton, New Jersey 08544

Y. W. Suen
Department of Electrical Engineering, Princeton University, Princeton, New Jersey 08544
and Department of Physics, National Chung-Hsing University, Taichung, Taiwan, Republic of China

H. C. Manoharan, X. Ying, M. B. Santos, and M. Shayegan
Department of Electrical Engineering, Princeton University, Princeton, New Jersey 08544

(Received 29 August 1994)

In bilayer electron systems realized in wide single quantum wells with intermediate density, we observe a many-body quantum Hall state at Landau-level filling $\nu=1$ stabilized by interlayer Coulomb interaction. This quantum Hall ground state makes a phase transition to a compressible state as density is increased. The unusual temperature and density dependence of the data as the transition boundary is approached is suggestive of an additional *finite-temperature* transition from a quantum Hall state to a compressible state, which is unique to bilayer systems.

Low-disorder bilayer electron systems (BLES's) exhibit unique quantum Hall phenomena such as a $\nu=\frac{1}{2}$ even-denominator fractional quantum Hall effect (QHE), which has no counterpart in single-layer two-dimensional electron systems (ν is the *total* filling factor for the BLES).[1–3] This QHE has been associated with a correlated, two-component Ψ_{331} Laughlin-like state stabilized by interlayer Coulomb interaction.[2–7] In BLES's with appropriate parameters, the interlayer interaction can also lead to *correlated* QHE at certain *integral* fillings such as $\nu=1$.[2,6–13] In contrast to the $\nu=1$ QHE state associated with the tunneling gap (Δ_{SAS}) separating the symmetric and antisymmetric states, the many-body, bilayer $\nu=1$ QHE state characterized by the two-component Ψ_{111} wave function has been predicted to exhibit properties such as neutral superfluid modes and a Kosterlitz-Thouless transition,[10,12,13] and has already revealed an unexpected in-plane field-driven phase transition (to another compressible state).[11–13]

We present here an experimental study of the $\nu=1$ QHE in BLES's in wide single quantum wells (WSQW's) of varying width and areal density N_S. The data reveal that the ground state at $\nu=1$ evolves continuously from a single-particle QHE state stabilized by a large Δ_{SAS} at low N_S to a many-body QHE state stabilized by strong interlayer interaction at intermediate N_S.[14] As N_S is further increased, we observe an incompressible-to-compressible transition. Near this transition, the many-body $\nu=1$ QHE state exhibits a remarkable dependence on temperature T: the diagonal resistivity becomes activated rather abruptly below a temperature (T^*) that strongly depends on N_S, while the measured quasiparticle excitation gaps are much larger than T^* and are nearly independent of N_S. As possible origins of this behavior, we discuss finite-T incompressible-to-compressible phase transitions that are unique to BLES's.

The samples are modulation-doped GaAs wells grown by molecular-beam epitaxy and have a width ranging from 680 to 1200 Å and typical low-T mobility $\sim 1\times 10^6$ cm^2/V s. They are of exceptionally high quality as they show very strong fractional QHE including quantum Hall states at the even denominator $\nu=\frac{1}{2}$ and $\frac{3}{2}$ fillings.[3] Front and back side gates were used to vary N_S and also to obtain symmetric charge distributions in the samples.[15] We measured Δ_{SAS} from the Fourier transform of the low-field magnetoresistance oscillations. The measured Δ_{SAS} were in excellent agreement with those determined from self-consistent Hartree-Fock calculations, an example of which is shown in Fig. 1(a) inset.

In a WSQW, increasing N_S leads to a reduction of Δ_{SAS} and an increase in d.[15] Here d is the calculated distance between electron layers [see inset to Fig. 1(a)]. We are therefore able to study the evolution of the ground state at $\nu=1$ in WSQW's as summarized in the d/l_B vs α [$=\Delta_{SAS}/(e^2/\varepsilon l_B)$] phase diagram of Fig. 1(a), where $l_B=(\hbar/eB)^{1/2}$ is the magnetic length. In this diagram the closed (open) symbols represent the presence (absence) of the $\nu=1$ QHE in WSQW's. For comparison, we have also indicated (shaded area) in Fig. 1(a) the region where the $\nu=\frac{1}{2}$ QHE is stable in the same or similar WSQW's.[3]

For an ideal BLES in which the thickness of the layers is zero, d/l_B is a measure of the competition between the intralayer and interlayer interaction, while α reflects the strength of the tunneling gap compared to the intralayer electron-correlation energy.[16] In systems with finite-layer thickness such as in wide parabolic wells[17] or WSQW's, however, the large layer thickness [λ in Fig. 1(a) inset] substantially reduces the short-range component of the Coulomb interaction and plays a crucial role in determining the ground state of the system. For example, as evident in Fig. 1(a) and discussed in detail elsewhere,[3] in WSQW's the $\nu=\frac{1}{2}$ QHE is observed at d/l_B values which far exceed the value $d/l_B\approx 2.5$ near which this state is theoretically expected[6,7] and experimen-

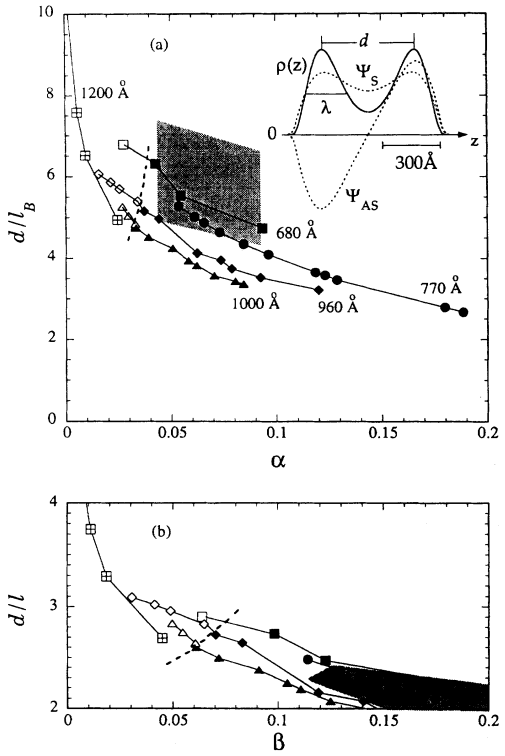

FIG. 1. In (a) experimental data are shown in d/l_B vs α $[=\Delta_{SAS}/(e^2/\varepsilon l_B)]$ phase diagram for BLES's in WSQW's at $\nu=1$. The closed (open) symbols represent the presence (absence) of $\nu=1$ QHE at the experimental base temperature of 25 mK. Data are shown for five WSQW samples with well widths between 680 and 1200 Å, and with varying areal densities; the solid thin curves are guides to the eye and go through data of a given sample. The dashed curve is the experimental transition boundary based on this data. The shaded area shows the region where a $\nu=\frac{1}{2}$ QHE is stable in BLES's in WSQW's. The inset exhibits the calculated electron wave functions (dotted curves denoted Ψ_S and Ψ_{AS}) and the distribution function [solid curve denoted $\rho(z)$] for a representative WSQW (width is 770 Å, $N_S=1.1\times10^{11}$ cm^{-2}) at $B=0$. In (b) the experimental data are shown in a d/l vs β $[=\Delta_{SAS}/(e^2/\varepsilon l)]$ phase diagram, where $l=(l_B^2+\lambda^2)^{1/2}$ is used to account for the effect of finite-layer thickness.

tally observed[2] to be stable in a BLES with small λ. In a crude approximation, replacing l_B by $l=(l_B^2+\lambda^2)^{1/2}$ to account for the finite-layer thickness[7] leads to the phase diagram of Fig. 1(b), which clearly demonstrates that both small tunneling *and* large effective layer separation are responsible for the collapse of the $\nu=1$ QHE in WSQW BLES's. The experimental boundary in Fig. 1(b) is qualitatively similar to the experimental and theoretical boundaries reported for the collapse of the $\nu=1$ QHE in BLES's in double quantum wells, where $\lambda\lesssim l_B$.[11,16,18] In the remainder of this paper we show that the $\nu=1$ QHE observed in WSQW's near the transition boundary, in approximately the same range of parameters where the many-body $\nu=\frac{1}{2}$ QHE state is stable, is also a many-body state, predominantly stabilized by strong interlayer correlations and possessing unusual finite-T properties.

We focus on data for one of our highest-quality samples, a 770-Å-wide quantum well that exhibits the strongest $\nu=\frac{1}{2}$

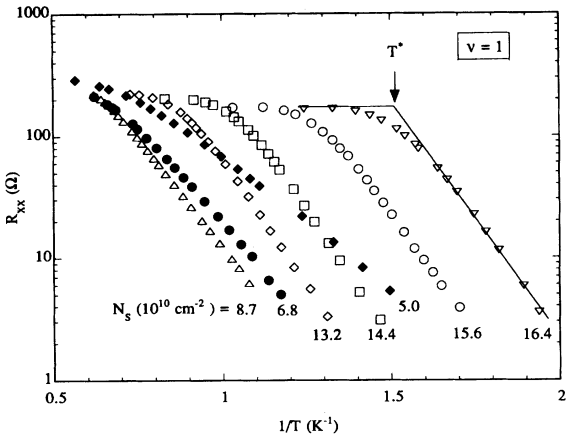

FIG. 2. Arrhenius plots of R_{xx} at $\nu=1$ vs $1/T$ for a WSQW of width 770 Å for different N_S. The temperature above which the activated behavior ends is marked by T^*.

and $\frac{3}{2}$ QHE in addition to the $\nu=1$ QHE.[3] Figure 2 presents Arrhenius plots of the diagonal resistance (R_{xx}) at $\nu=1$ for electron density $5.0\leq N_S\leq16.4\times10^{10}$ cm^{-2} experimentally achievable in this sample. The quasiparticle excitation gaps $^1\Delta$ determined from the slopes of the activated regions of these plots according to $R_{xx}\sim\exp(-{}^1\Delta/2T)$, together with the measured and calculated Δ_{SAS}, are shown in Fig. 3(a) as a function of N_S. Several features of the data of Figs. 2 and 3 are particularly noteworthy: (1) While Δ_{SAS} decreases with increasing N_S, $^1\Delta$ increases and exceeds Δ_{SAS} by more than

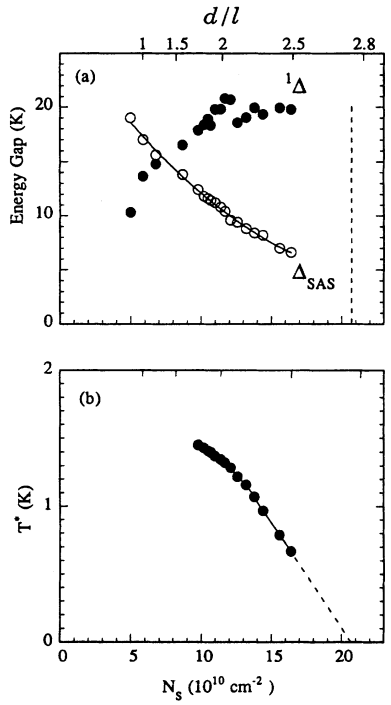

FIG. 3. (a) Measured Δ_{SAS} and $^1\Delta$ energy gaps for the $\nu=1$ QHE as a function of N_S (lower axis) or d/l (top axis) for a 770-Å-wide WSQW. The solid curve is the calculated Δ_{SAS}. (b) Plot of experimental T^* vs N_S and d/l.

a factor of 3 at the highest accessible N_S. (2) For $N_S \gtrsim 10\times10^{10}$ cm^{-2}, the activated behavior of R_{xx} vs $1/T$ starts rather abruptly below an N_S-dependent temperature T^*. Above T^*, the R_{xx} minimum at $\nu=1$ vanishes, i.e., R_{xx} is nearly independent of magnetic field and T. For $N_S \lesssim 10\times10^{10}$ cm^{-2}, the Arrhenius plots show a smoother behavior and $^1\Delta$ gaps start to decrease with decreasing N_S. (3) The measured $^1\Delta$ for $N_S > 10\times10^{10}$ cm^{-2} are approximately constant ($\approx$20 K) and exceed T^* by more than an order of magnitude. (4) The plot of the measured T^* vs N_S presented in Fig. 3(b) shows that T^* decreases with increasing N_S and extrapolates to zero at $N_S = 20.5\times10^{10}$ cm^{-2}. This N_S corresponds to $\beta=0.073$ and $d/l=2.75$, consistent with the phase boundary of Fig. 1(b). These features clearly point to the many-body origin of the $\nu=1$ QHE states observed at large N_S in this WSQW.

The data of Figs. 1–3 demonstrate that the ground state of the BLES's in WSQW's at $\nu=1$ evolves continuously from a single-particle QHE at low N_S, where the tunneling (Δ_{SAS}) is large, to a many-body QHE state at intermediate N_S, and then makes a transition to a metallic state at large N_S. We believe that in the intermediate N_S range we are observing a bilayer QHE state stabilized by comparable interlayer and intralayer correlations. A possible candidate is the two-component Ψ_{111} state, which, for a BLES with negligible layer thickness and interlayer tunneling, is predicted to be stable for $d/l_B \approx 2$.[6–10,13] This state has been discussed widely and may be responsible for some of the $\nu=1$ QHE states reported in the double-quantum-well samples of Ref. 11. The observation of a Ψ_{111}-like state in our WSQW's with such a large d/l_B may initially seem surprising. As already pointed out, however, in our system, the short-range component of the *intralayer* Coulomb interaction is softened because of the large electron layer thickness (typically $\lambda/l_B \sim 2$). It is therefore reasonable that the Ψ_{111} state in our system would be stable under the conditions of reduced *interlayer* correlation (i.e., larger d/l_B). Consistent with this conjecture, Fig. 1(b) shows that, if corrections for the finite-layer thickness are made, the effective layer separation (d/l) in our WSQW's at intermediate N_S are indeed close to the predicted value for the stability of the Ψ_{111} state. Finally, as mentioned earlier, in these WSQW's we also observe a strong $\nu=\frac{1}{2}$ fractional QHE state that we can associate with another two-component (Ψ_{331}) state with comparable interlayer and intralayer correlations.[3] The stability of the $\nu=\frac{1}{2}$ and the many-body $\nu=1$ QHE states in a similar range of d/l vs β diagram [see Fig. 1(b)] suggests that the latter is also a correlated bilayer state. We note that for small β and large d/l, the $\nu=\frac{1}{2}$ QHE also collapses, but it makes a transition to an insulating phase rather than a metallic phase.[3,19]

Data on another WSQW with a well width of 1000 Å, in which we can cross the boundary for the collapse of the $\nu=1$ QHE (see Fig. 1), are similar to and consistent with the results presented here. For large N_S ($d/l > 2.6$), the 1000-Å-wide sample shows a metallic behavior (R_{xx} nearly independent of T) at $\nu=1$ down to our base T of 25 mK and there is no signature of a $\nu=1$ QHE minimum. For intermediate N_S, at high temperature R_{xx} at $\nu=1$ nearly coincides with the high N_S (metallic) data, but below an N_S-dependent T^* a $\nu=1$ QHE abruptly develops and quickly becomes activated.

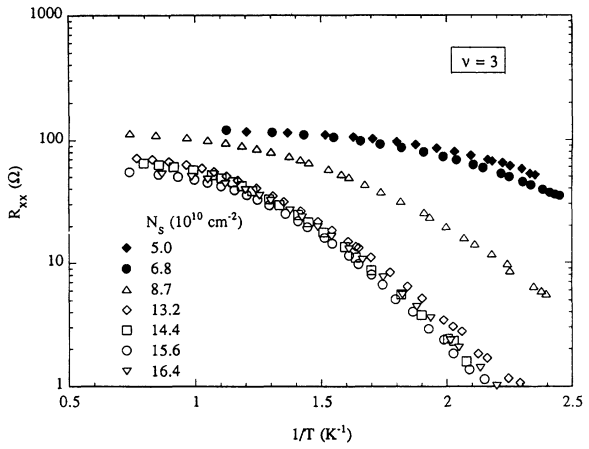

FIG. 4. Arrhenius plots of R_{xx} at $\nu=3$ vs $1/T$ for the sample of Fig. 2.

The dependence of T^* on N_S is similar to the data shown in Fig. 3(b) and, in particular, T^* decreases with increasing N_S (increasing d/l) and tends towards zero as $d/l \to 2.6$, consistent with the phase boundary of Fig. 1(b). For very small N_S, similar to the data of Fig. 2, no clear T^* is observed and the high-T data deviate from the high-N_S metallic data.

The data of Figs. 2 and 3 are collectively very unusual and qualitatively different from what is observed for the integral or fractional QHE in standard single-layer two-dimensional (2D) systems or for the QHE at higher fillings such as $\nu=3$ in the *same* BLES sample (Fig. 4). As N_S is lowered, the single-layer $\nu=1$ QHE data[20] exhibit a larger R_{xx} (at any given T), a smaller excitation gap, and typically a smoother saturation of the activated behavior at high T.[21] This behavior is very similar to what we observe for the $\nu=3$ QHE in our sample (Fig. 4) and for the $\nu=1$ QHE at *low* N_S ($<10\times10^{10}$ cm^{-2}) far away from the compressible boundary (Fig. 2). It is in sharp contrast to the $\nu=1$ data at *high* N_S near the compressible boundary ($N_S > 10\times10^{10}$ cm^{-2} in Fig. 2), where R_{xx} vs T^{-1} data appear to simply shift horizontally to *lower* T as N_S is *raised*.

Based on what is known for the QHE in single-layer 2D systems, our experimental observations and, in particular, the dependence of T^* on N_S near the compressible boundary remain unexplained. Our data appear to be consistent, on the other hand, with the signatures of a Kosterlitz-Thouless (KT) transition that has been recently proposed for BLES's.[10,13] Associating the layer population with an isospin, the theories argue that in the limit of zero interlayer separation ($d=0$), the spin system has the symmetry of the 2D quantum ferromagnetic Heisenberg model. For finite d and in the absence of interlayer tunneling,[22] however, the system has an XY symmetry and thus may support a KT transition at a critical temperature T_{KT}. As the effective layer separation becomes larger, T_{KT} decreases and vanishes above a critical separation.[13] The manifestation of this KT transition in the transport coefficients of the BLES is not entirely clear, although it is predicted that below T_{KT} a gap for the creation of charged particle-hole pairs should lead to a QHE with an activated resistivity.[13] Associating our observed T^* with T_{KT}, the data of Figs. 2 and 3 are qualitatively consistent

with these predicted features: we observe a QHE for $T<T^*$, our measured T^* are of the order of the rough estimates given for T_{KT}, and both T^* and T_{KT} decrease with increasing d/l.

An alternative explanation for our data may be the following.[23] Consider the BLES at $T=0$ at an N_S where $\nu=1$ QHE is observed, but close to the boundary for its collapse. Two possible states for the system are (1) a correlated (Ψ_{111}-like) incompressible QHE state, and (2) an uncorrelated compressible state with $\nu=\frac{1}{2}$ in each layer. The correlated state, being energetically more favorable, is the ground state. The uncorrelated state, however, has larger entropy. It is therefore possible that the BLES makes a transition from the correlated QHE to the uncorrelated (compressible) state at finite T. This is qualitatively consistent with our observation that the closer the BLES is to the compressible boundary the smaller the T needed to destroy the correlated QHE state (Fig. 3). For an ideal BLES, such a transition should be first order and one may expect sharper features in the R_{xx} vs $1/T$ data than observed in Fig. 2. Sample impurities and inhomogeneity, however, may lead to a smoother transition, consistent with the experimental data.

In summary, we have presented ground-state and finite-T data for the $\nu=1$ QHE in BLES's in WSQW's. The results provide evidence for the presence of many-body integral QHE in these systems, and point to the rich and not yet understood transitions brought about by the interplay of intralayer and interlayer correlations *and* temperature.

We thank S. M. Girvin, F. D. M. Haldane, A. H. MacDonald, I. A. McDonald, K. Moon, D. C. Tsui, X. G. Wen, and K. Yang for useful discussions and D. Shahar and L. W. Engel for technical assistance. H.C.M. thanks the Fannie and John Hertz Foundation for financial support. This work was supported in part by the NSF, Grants Nos. DMR-9222418 and DMR-9224077.

[1] Y. W. Suen, L. W. Engel, M. B. Santos, M. Shayegan, and D. C. Tsui, Phys. Rev. Lett. **68**, 1379 (1992).

[2] J. P. Eisenstein, G. S. Boebinger, L. N. Pfeiffer, and S. He, Phys. Rev. Lett. **68**, 1383 (1992).

[3] Y. W. Suen, H. C. Manoharan, X. Ying, M. B. Santos, and M. Shayegan, Phys. Rev. Lett. **72**, 3405 (1994).

[4] B. I. Halperin, Helv. Phys. Acta **56**, 75 (1983).

[5] E. H. Rezayi and F. D. M. Haldane, Bull. Am. Phys. Soc. **32**, 892 (1987).

[6] D. Yoshioka, A. H. MacDonald, and S. M. Girvin, Phys. Rev. B **39**, 1932 (1989); S. He, X. C. Xie, S. Das Sarma, and F. C. Zhang, *ibid.* **43**, 9339 (1991).

[7] S. He, S. Das Sarma, and X. C. Xie, Phys. Rev. B **47**, 4394 (1993).

[8] T. Chakraborty and P. Pietilainen, Phys. Rev. Lett. **59**, 2784 (1987).

[9] H. A. Fertig, Phys. Rev. B **40**, 1087 (1989).

[10] X. G. Wen and A. Zee, Phys. Rev. Lett. **69**, 1811 (1992).

[11] S. Q. Murphy, J. P. Eisenstein, G. S. Boebinger, L. N. Pfeiffer, and K. W. West, Phys. Rev. Lett. **72**, 728 (1994).

[12] Z. F. Ezawa and A. Iwazaki, Int. J. Mod. Phys. B **6**, 3205 (1992); **8**, 2111 (1994), and references therein.

[13] K. Yang, K. Moon, L. Zheng, A. H. MacDonald, S. M. Girvin, D. Yoshioka, and S.-C. Zhang, Phys. Rev. Lett. **72**, 732 (1994); K. Moon, H. Mori, K. Yang, S. M. Girvin, A. H. MacDonald, L. Zheng, D. Yoshioka, and S.-C. Zhang (unpublished).

[14] A similar continuous evolution was also concluded in Ref. 11 based on data for BLES's in double quantum wells.

[15] Y. W. Suen, J. Jo, M. B. Santos, L. W. Engel, S. W. Hwang, and M. Shayegan, Phys. Rev. B **44**, 5974 (1991).

[16] A. H. MacDonald, P. M. Platzman, and G. S. Boebinger, Phys. Rev. Lett. **65**, 775 (1990).

[17] M. Shayegan, J. Jo, Y. W. Suen, M. B. Santos, and V. J. Goldman, Phys. Rev. Lett. **65**, 2916 (1990); S. He, F. C. Zhang, X. C. Xie, and S. Das Sarma, Phys. Rev. B **42**, 11 376 (1990).

[18] G. S. Boebinger, H. W. Jiang, L. N. Pfeiffer, and K. W. West, Phys. Rev. Lett. **64**, 1793 (1990).

[19] Y. W. Suen, M. B. Santos, and M. Shayegan, Phys. Rev. Lett. **69**, 3551 (1992).

[20] See, e.g., A. Usher, R. J. Nicholas, J. J. Harris, and C. T. Foxon, Phys. Rev. B **41**, 1129 (1990).

[21] For the particular case of a single-layer $\nu=1$ QHE arising from the exchange-enhanced Zeeman gap, a saturation of the Arrhenius resistivity plots above a T, which is often smaller than the excitation gap, has been reported (see, e.g., Ref. 20). This saturation can be attributed to a rapid loss of the ferromagnetic order and the collapse of the energy gap with increasing T. Similar to the $\nu=3$ results of Fig. 4, however, the single-layer $\nu=1$ data typically exhibit a smoother saturation and, more importantly, do not show the intriguing N_S dependence that the $\nu=1$ data of Fig. 2 exhibit.

[22] In the presence of finite but small tunneling, the KT transition may turn into a rapid crossover. This is not inconsistent with the data presented here. Also, since tunneling in WSQW's depends on the self-consistent charge distribution in the well and therefore on exchange and correlation, it is possible that in the presence of a large magnetic field the tunneling in WSQW's is substantially modified and possibly reduced.

[23] X. G. Wen (private communication).

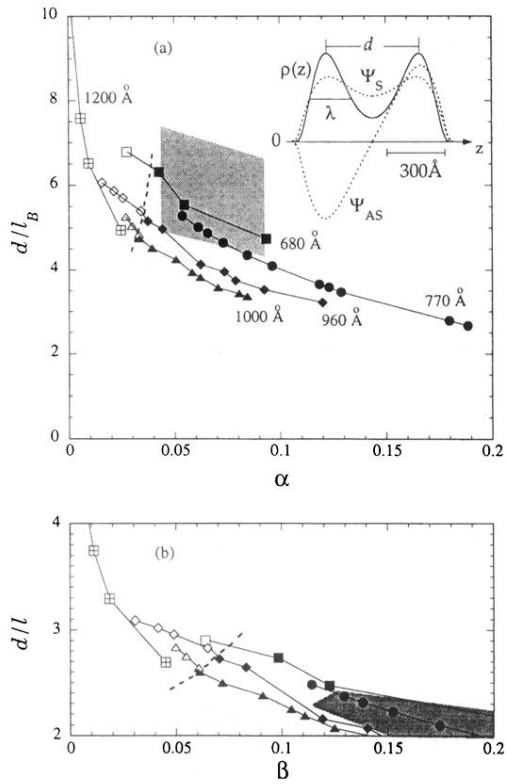

FIG. 1. In (a) experimental data are shown in d/l_B vs α $[=\Delta_{\mathrm{SAS}}/(e^2/\varepsilon l_B)]$ phase diagram for BLES's in WSQW's at $\nu=1$. The closed (open) symbols represent the presence (absence) of $\nu=1$ QHE at the experimental base temperature of 25 mK. Data are shown for five WSQW samples with well widths between 680 and 1200 Å, and with varying areal densities; the solid thin curves are guides to the eye and go through data of a given sample. The dashed curve is the experimental transition boundary based on this data. The shaded area shows the region where a $\nu=\frac{1}{2}$ QHE is stable in BLES's in WSQW's. The inset exhibits the calculated electron wave functions (dotted curves denoted Ψ_S and Ψ_{AS}) and the distribution function [solid curve denoted $\rho(z)$] for a representative WSQW (width is 770 Å, $N_S=1.1\times10^{11}$ cm^{-2}) at $B=0$. In (b) the experimental data are shown in a d/l vs β $[=\Delta_{\mathrm{SAS}}/(e^2/\varepsilon l)]$ phase diagram, where $l=(l_B^2+\lambda^2)^{1/2}$ is used to account for the effect of finite-layer thickness.